

Investigation of extra traps measured by charge pumping technique in high voltage zone in p-channel metal-oxide-semiconductor field-effect transistors with HfO₂/metal gate stacks

Szu-Han Ho, Ting-Chang Chang, Bin-Wei Wang, Ying-Shin Lu, Wen-Hung Lo, Ching-En Chen, Jyun-Yu Tsai, Hua-Mao Chen, Guan-Ru Liu, Tseung-Yuen Tseng, Osbert Cheng, Cheng-Tung Huang, and Xi-Xin Cao

Citation: [Applied Physics Letters](#) **102**, 012106 (2013); doi: 10.1063/1.4773914

View online: <http://dx.doi.org/10.1063/1.4773914>

View Table of Contents: <http://scitation.aip.org/content/aip/journal/apl/102/1?ver=pdfcov>

Published by the [AIP Publishing](#)

Articles you may be interested in

[Abnormal threshold voltage shift under hot carrier stress in Ti_{1-x}N_x/HfO₂ p-channel metal-oxide-semiconductor field-effect transistors](#)

J. Appl. Phys. **114**, 124505 (2013); 10.1063/1.4822158

[Investigation of an anomalous hump in gate current after negative-bias temperature-instability in HfO₂/metal gate p-channel metal-oxide-semiconductor field-effect transistors](#)

Appl. Phys. Lett. **102**, 012103 (2013); 10.1063/1.4773479

[Analysis of anomalous traps measured by charge pumping technique in HfO₂/metal gate n-channel metal-oxide-semiconductor field-effect transistors](#)

Appl. Phys. Lett. **101**, 233509 (2012); 10.1063/1.4769444

[Analysis of an anomalous hump in gate current after dynamic negative bias stress in Hf_xZr_{1-x}O₂/metal gate p-channel metal-oxide-semiconductor field-effect transistors](#)

Appl. Phys. Lett. **101**, 052105 (2012); 10.1063/1.4739525

[Anomalous negative bias temperature instability behavior in p-channel metal-oxide-semiconductor field-effect transistors with Hf Si O N Si O₂ gate stack](#)

Appl. Phys. Lett. **90**, 233505 (2007); 10.1063/1.2745649



NEW! Asylum Research MFP-3D Infinity™ AFM
Unmatched Performance, Versatility and Support

OXFORD INSTRUMENTS
The Business of Science®

Stunning high performance
Simpler than ever to GetStarted™
Comprehensive tools for nanomechanics
Widest range of accessories for materials science and bioscience

The advertisement features several images: a blue textured surface, a brown textured surface, a yellow and red patterned surface, a set of colorful rectangular samples, and the Asylum Research MFP-3D Infinity AFM instrument.

Investigation of extra traps measured by charge pumping technique in high voltage zone in p-channel metal-oxide-semiconductor field-effect transistors with HfO₂/metal gate stacks

Szu-Han Ho,¹ Ting-Chang Chang,^{2,a)} Bin-Wei Wang,³ Ying-Shin Lu,² Wen-Hung Lo,² Ching-En Chen,¹ Jyun-Yu Tsai,² Hua-Mao Chen,⁴ Guan-Ru Liu,² Tseung-Yuen Tseng,¹ Osbert Cheng,⁵ Cheng-Tung Huang,⁵ and Xi-Xin Cao³

¹Department of Electronics Engineering, National Chiao Tung University, Hsinchu 300, Taiwan

²Department of Physics, National Sun Yat-Sen University, Kaohsiung 804, Taiwan

³Department of Electronics Engineering, Peking University, Beijing 100871, China

⁴Department of Photonics & Institute of Electro-Optical Engineering, National Chiao Tung University, Hsinchu, Taiwan

⁵Device Department, United Microelectronics Corporation, Tainan Science Park, Taiwan

(Received 9 November 2012; accepted 17 December 2012; published online 8 January 2013)

This letter investigates extra traps measured by charge pumping technique in the high voltage zone in p-channel metal-oxide-semiconductor field-effect transistors with HfO₂/metal gate stacks. N - $V_{\text{high level}}$ characteristic curves with different duty ratios show that the hole discharge time ($t_{\text{base level}}$) dominates the value of extra traps. By fitting $\ln(N(t_{\text{base level}} = 1\mu\text{s}) - N(t_{\text{base level}})) - \Delta t_{\text{base level}}$ at different temperatures and computing the equation $t = \tau_0 \exp(\alpha_{\text{h,SiO}_2} d_{\text{SiO}_2} + \alpha_{\text{h,HfO}_2} d_{\text{HfO}_2,\text{trap}})$, the results show that these extra traps measured by the charge pumping technique at high voltage zone can be attributed to high-k bulk shallow traps. © 2013 American Institute of Physics. [<http://dx.doi.org/10.1063/1.4773914>]

With the scaling down of metal-oxide semiconductor field-effect transistors (MOSFETs), conventional SiO₂-based dielectric is only a few atomic layers thick, causing gate current to rise, power dissipation to increase, and performance to degrade. Besides, conventional SiO₂-based dielectrics have approached their physical limits. Hence, replacing SiO₂-based dielectrics with high-k based dielectrics is a valid solution to these problems. In addition, high-k/metal gates can be integrated with techniques such as silicon on insulator (SOI),¹⁻³ strained-silicon,^{4,5} and multi-gate to improve device characteristics. As recommended in the International Technology Roadmap for Semiconductors, Hf-based dielectrics have been heavily studied to replace SiO₂-based dielectrics in recent years.⁶⁻⁹ However, with changes in Hf-based dielectrics, many measurement techniques must be corrected, especially charge pumping techniques. For instance, with a decrease in frequency, charge pumping current (I_{cp}) decreases in conventional SiO₂-based dielectrics since carriers have enough time to discharge from interface shallow traps. Conversely, with a decrease in frequency, I_{cp} increases in Hf-based dielectrics since carriers have enough time to tunnel into high-k bulk traps.¹⁰ Charge pumping techniques play an important role in inspecting defects. Thus, this study mainly focuses on extra traps measured by the charge pumping technique at high voltage, with the devices used in this study HfO₂ dielectric p-channel MOSFETs (p-MOSFETs). The causes of the extra traps are explained in this letter.

The HfO₂/metal gate p-MOSFETs used in this study were fabricated by the gate-first process. First, a high quality 1 nm-thick thermal oxide was grown as an interfacial layer. Second, 3 nm of HfO₂ dielectrics were sequentially deposited by atomic layer deposition. Third, 10 nm of Ti_xN_{1-x} was

deposited by radio frequency physical vapor deposition because metal gates can eliminate gate depletion and resist remote phonon scattering.^{11,12} Next, poly-Si was deposited as a low resistance gate electrode. Finally, the dopant activation was performed at 1025 °C. The p-MOSFETs were measured by the charge pumping technique with different duty ratios at different temperatures. A pulse train with low-voltage of 1 V, high-voltage from 0 V to -1.29 V, and frequency of 200 kHz was applied on the gate terminal. $I_{\text{g}}-V_{\text{g}}$ transfer curves were measured with the source, drain, and body terminals all grounded, with V_{g} given from 0 V to -1.29 V. Then through body floating (BF), source/drain floating (SDF), and source/drain/body all grounded (SDB) process, the current path and carrier polarity can be confirmed. Next, the $I_{\text{g}}-V_{\text{g}}$ curve is fitted by Frenkel-Poole mechanism and tunneling mechanism. All experimental curves were measured using an Agilent B1500 semiconductor parameter analyzer.

Figure 1 shows the N - $V_{\text{high level}}$ characteristic curves at different duty ratios. N is the number of traps, and duty ratio = ($t_{\text{high level}}/t_{\text{cycle}}$). Clearly, N - $V_{\text{high level}}$ characteristic curves are the same at $V_{\text{high level}} < |-0.8\text{V}|$ with an increase in duty ratio. This is because the time for holes in the interface traps to recombine with electrons is very short. Hence, the number of interface traps measured by I_{cp} is not sensitive to duty ratio. On the contrary, N decreases with a rise in duty ratio for $V_{\text{high level}} > |-0.8\text{V}|$. Furthermore, only interface traps can be measured with a duty ratio value of 97.5%. In other words, extra traps nearly disappear. The detrapping time ($t_{\text{base level}}$) of holes dominates the value of N such that N becomes smaller with a decrease in the detrapping time. This result demonstrates that holes need time to discharge. Thus, it is necessary to know the relationship between N and the detrapping time ($t_{\text{base level}}$) for $V_{\text{high level}} > |-0.8\text{V}|$. The inset of

^{a)}Electronic mail: tcchang@mail.phys.nsysu.edu.tw.

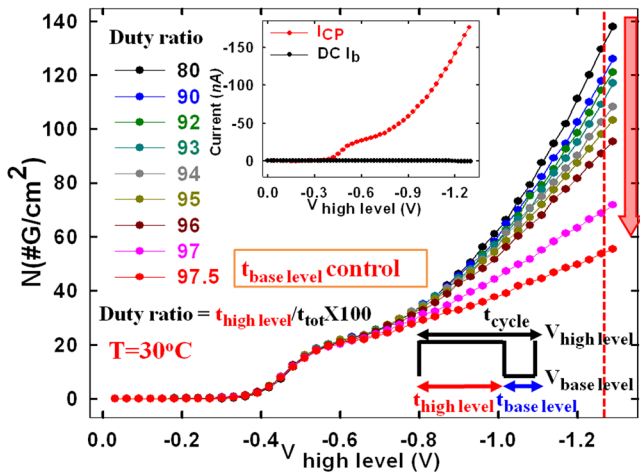


FIG. 1. N - $V_{\text{high level}}$ characteristic curves at different duty ratios by charge pumping measurement. Inset shows I - $V_{\text{high level}}$ curve with source, drain and body all grounded.

Fig. 1 shows I - $V_{\text{high level}}$ curves with source, drain, and body all grounded. It can be first observed that body current (I_b) is much smaller than I_{cp} . In addition, $N(I_{cp})$ is dependent on the detrapping time. Hence, these results indicate that N measured by the charge pumping technique is caused by high- k bulk traps rather than gate leakage current.

The inset of Figure 2 shows the N - $t_{\text{base level}}$ curve at 30°C , for $V_g = V_t - 0.7\text{V}$, shown by the dotted red line in Fig. 1. Since N can also represent the number of holes discharged from high- k bulk traps, $N(t_{\text{base level}} = 1\ \mu\text{s}) - N(t_{\text{base level}})$ is the number of holes still charged in the high- k bulk traps at $t_{\text{base level}}$, an important parameter. Figure 2 shows $\ln(N(t_{\text{base level}} = 1\ \mu\text{s}) - N(t_{\text{base level}})) - \Delta t_{\text{base level}}$ curves fitted from the inset of Figure 2. $\Delta t_{\text{base level}}$ is $t_{\text{base level}} - t_{\text{base level}}$ (125 ns). $\Delta t_{\text{base level}}$ is the time for holes to discharge from traps. Clearly, fitting these curves can be accomplished with straight lines even for different temperatures (30°C - 90°C). In addition, slopes are also similar at these temperatures. The discharge equation can be described by $dQ(t)/dt = -\Delta Q(t)/\tau_p = -e_p \Delta Q(t)$, $\Delta Q(t) = \Delta Q(0)\exp(-e_p t)$,¹³ where e_p is the escape probability,

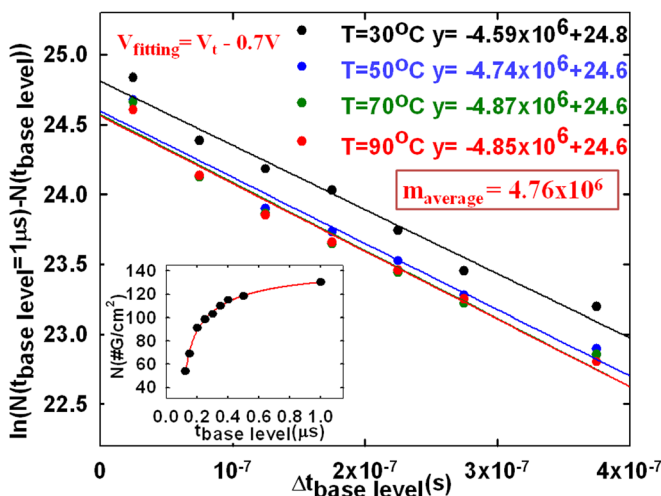


FIG. 2. $\ln(N(t_{\text{base level}} = 1\ \mu\text{s}) - N(t_{\text{base level}})) - \Delta t_{\text{base level}}$ curves at different temperatures at $V_g = V_t - 0.7\text{V}$. Inset shows N - $t_{\text{base level}}$ curve at 30°C for $V_g = V_t - 0.7\text{V}$.

and τ_p is the average escape time. Thus, slope is indicated by e_p or $1/\tau_p$ with e_p not dependent on temperature. Hence, e_p is the tunneling probability. The average value of the slope at different temperatures (m_{average}) is 4.76×10^6 , and $\tau_{p,\text{average}}$ is 2.1×10^{-7} (s). Now the value of tunneling distance can be determined by using $\tau_{p,\text{average}}$ and can verify that the traps are actually in the high- k bulk. The relationship between tunneling time and distance can be approximated by $t = \tau_0 \exp(\alpha_h x)$, $\alpha_h = 2(2m_h q \phi_0 / \hbar^2)^{0.5}$,^{14,15} where τ_0 is hole tunneling characteristic time, m_h is hole effective mass for SiO_2 , and $q\phi_0$ is an effective tunneling barrier height. However, because holes are tunneling through two layers, SiO_2 and HfO_2 , this equation can be described by $t = \tau_0 \exp(\alpha_{h,\text{SiO}_2} d_{\text{SiO}_2} + \alpha_{h,\text{HfO}_2} d_{\text{HfO}_2,\text{trap}})$, $\alpha_{h,\text{SiO}_2} = 2(2m_{h,\text{SiO}_2} q \phi_{0,\text{SiO}_2} / \hbar^2)^{0.5}$, and $\alpha_{h,\text{HfO}_2} = 2(2m_{h,\text{HfO}_2} q \phi_{0,\text{HfO}_2} / \hbar^2)^{0.5}$, where d_{SiO_2} is the thickness of SiO_2 , $d_{\text{HfO}_2,\text{trap}}$ is the distance from traps to interlayer between SiO_2 and HfO_2 , m_{h,SiO_2} and m_{h,HfO_2} are effective mass in SiO_2 and HfO_2 , respectively, and $q\phi_{0,\text{SiO}_2}$ and $q\phi_{0,\text{HfO}_2}$ are effective tunneling barrier height in SiO_2 and HfO_2 , respectively. Values for τ_0 , m_{h,SiO_2} , and m_{h,HfO_2} can be obtained from other research.^{14,16,17} Thus, only one parameter (ϕ_{0,HfO_2}) is unknown.

The inset in Figure 3(a) shows I_g - V_g characteristic curves with BF, SDF, and SDB for distinguishing gate current at 30°C . Clearly, the I_g - V_g characteristic curve in BF is similar to that in SDB, and the I_g - V_g characteristic curve in SDF is much smaller than either. These results indicate that holes transfer from source/drain to the gate, rather than electrons transferring from gate to body. Clearly, section A indicates the tunneling current in Fig. 3(b), from $V_g = -0.26\text{V}$ to $V_g = -0.42\text{V}$, while section B is Frenkel-Poole current, shown in the inset of Fig. 3(d), from $V_g = -0.94\text{V}$ to $V_g = -1.29\text{V}$. The parameter $\phi_B = 0.244\text{eV}$ can be obtained by fitting the Frenkel-Poole mechanism in the inset in Fig. 3(d).¹⁸⁻²⁰ Figure 3(c) shows the N - $V_{\text{high level}}$ characteristic curves at different duty ratios. When $V_g < |-0.8\text{V}|$, N is interface traps (N_{it}) only. On the contrary, when $V_g > |-0.8\text{V}|$, N is both high- k bulk shallow traps (N_{hkst}) and N_{it} . A comparison of Fig. 3(c) with Fig. 3(a) shows that N is only N_{it} when gate current is tunneling current and Frenkel-Poole current is very small. Conversely, N is both N_{it} and N_{hkst} when gate current is Frenkel-Poole current. This indicates that bulk traps charging holes via the Frenkel-Poole mechanism and the traps discharging holes through I_{cp} may be the same. In order to confirm this theory, $\phi_B = \phi_{0,\text{HfO}_2} = 0.244\text{eV}$ is substituted into the equation $t = \tau_0 \exp(\alpha_{h,\text{SiO}_2} d_{\text{SiO}_2} + \alpha_{h,\text{HfO}_2} d_{\text{HfO}_2,\text{trap}})$, with $\alpha_{h,\text{SiO}_2} = 2(2m_{h,\text{SiO}_2} q \phi_{0,\text{SiO}_2} / \hbar^2)^{0.5}$, and $\alpha_{h,\text{HfO}_2} = 2(2m_{h,\text{HfO}_2} q \phi_{0,\text{HfO}_2} / \hbar^2)^{0.5}$, where m_{h,SiO_2} is $0.32m_0$, m_{h,HfO_2} is $0.85m_0 \sim 1.28m_0$, $\tau_0 = 6.6 \times 10^{-14}$ (s), d_{SiO_2} is 10\AA , and $\phi_{0,\text{SiO}_2} = 1.4\text{eV} + \phi_{0,\text{HfO}_2}$. Finally, $d_{\text{HfO}_2,\text{trap}}$ is calculated as $13.2\text{\AA} - 16.2\text{\AA}$. This is a reasonable value. While V_g transits from $V_{\text{high level}}$ to $V_{\text{base level}}$, holes in the high- k bulk shallow traps near the gate and substrate discharge to gate and source/drain, respectively. Hence, only traps in the middle of the high- k bulk shallow traps can be measured by the charge pumping technique. In addition, the falling time is 1.25×10^{-7} (s), which matches the hole discharge time at duty ratio of 97.5%, that of 1.25×10^{-7} (s). This implies that holes in the middle of the high- k bulk shallow traps have no time to tunnel to the substrate in the accumulation area. Thus, only interface traps can be measured by I_{cp} at a duty ratio value of 97.5%.

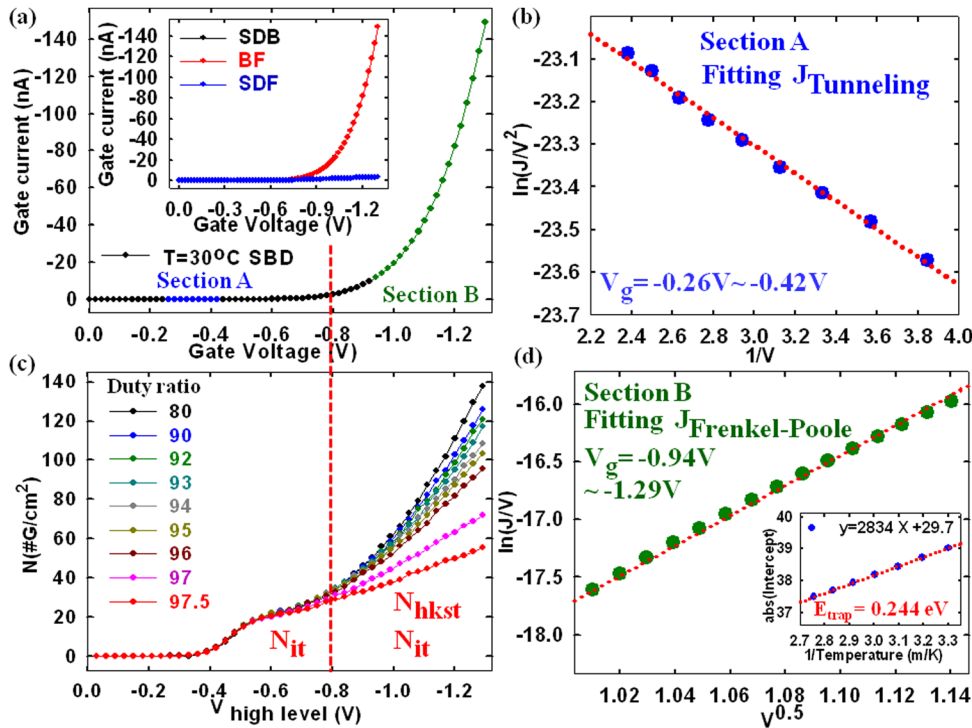


FIG. 3. (a) I_g - V_g characteristic curves with SDB. Inset shows I_g - V_g characteristic curves with BF, SDF, and SDB. (b) Gate current in section A is fitted by tunneling model. (c) N - $V_{\text{high level}}$ characteristic curves with different duty ratios for charge pumping measurement. (d) Gate current in section B is fitted by Frenkel-Poole model.

Combining the results above, the energy band diagram of the model for charge pumping measurement with anomalous traps can be acquired, as shown in Fig. 4. Figures 4(a) and 4(b) show the energy band diagram when pulses are applied to the gate with the charge pumping technique at high and base levels, respectively. When $|-0.8V| > V_{\text{high level}} > V_t$, gate current is tunneling-path dominated, leading to high-k bulk shallow traps not charging holes. Holes merely charge to interface traps, as shown in Fig. 4(a). Subsequently, holes recombine with electrons in the interface traps at $V_{\text{base level}}$, as shown in Fig. 4(b). Thus, I_{cp} only

detects N_{it} . On the contrary, when $V_g > |-0.8V|$, the gate current is dominated by the Frenkel-Poole mechanism, causing high-k bulk shallow traps to charge holes. Next, holes charge in interface traps and high-k bulk shallow traps, as shown in Fig. 4(c). Then holes recombine with electrons in the interface traps at $V_{\text{base level}}$, and holes discharge from high-k bulk shallow traps to the body by the tunneling mechanism. Therefore, I_{cp} measures not only interface traps, N_{it} , but also high-k bulk shallow traps.

In summary, N - $V_{\text{high level}}$ characteristic curves are nearly the same in value for $V_{\text{high level}} < |-0.8V|$ with a rise

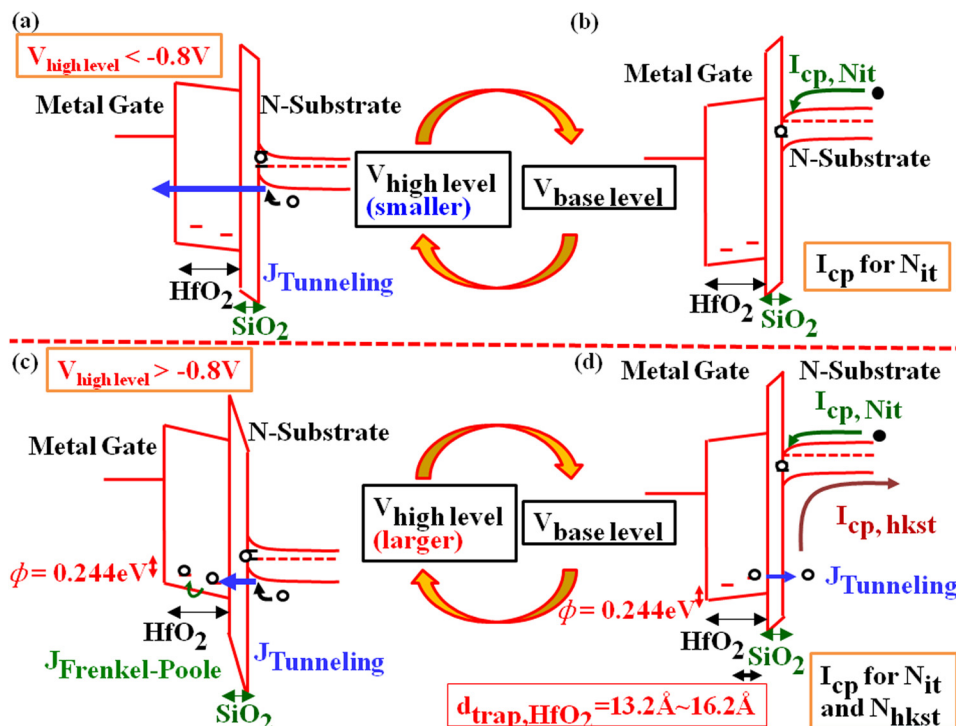


FIG. 4. The energy band diagram of high-k/metal gate MOSFETs with charge pumping measurement (a) at $V_{\text{high level}} < |-0.8V|$ and (b) at $V_{\text{base level}}$, where $V_{\text{high level}} < |-0.8V|$. The energy band diagram of high-k/metal gate MOSFETs with charge pumping measurement (c) at $V_{\text{high level}}$ and (d) at $V_{\text{base level}}$, where $V_{\text{high level}} > |-0.8V|$.

in duty ratio. However, N decreases with an increase in duty ratio for $V_{\text{high level}} > |-0.8\text{V}|$. This indicates that the discharge time dominates the value of N . In addition, the values of e_p obtained by the slope of $\ln(N(t_{\text{base level}} = 1 \mu\text{s}) - N(t_{\text{base level}})) - \Delta t_{\text{base level}}$ are independent of temperature. Hence, holes discharge from high- k bulk shallow traps via the tunneling mechanism. The distance of traps can be acquired by the equation $t = \tau_0 \exp(\alpha_{\text{h,SiO}_2} d_{\text{SiO}_2} + \alpha_{\text{h,HfO}_2} d_{\text{HfO}_2, \text{trap}})$ with $\phi_{0, \text{HfO}_2} = 0.244 \text{ eV}$ and ϕ_{0, SiO_2} obtained from fitting the gate current with the Frenkel-Poole mechanism. From this, $d_{\text{HfO}_2, \text{trap}}$ can be calculated as $13.2 \text{ \AA} - 16.2 \text{ \AA}$, a reasonable value. This result is proof that traps are actually located in the high- k shallow bulk. This study shows that extra traps measured by the charge pumping technique in a $\text{HfO}_2/\text{metal gate p-MOSEFTs}$ at high gate voltage can be attributed to high- k bulk shallow traps.

Part of this work was performed at United Microelectronics Corporation. The work was supported by the National Science Council under Contract No. NSC 101-2120-M-110-002.

¹C. H. Dai, T. C. Chang, A. K. Chu, Y. J. Kuo, S. C. Chen, C. T. Tsai, W. H. Lo, S. H. Ho, G. Xia, O. Cheng *et al.*, *Surf. Coat. Technol.* **205**, 1470–1474 (2010).

²C. H. Dai, T. C. Chang, A. K. Chu, Y. J. Kuo, F. Y. Jian, W. H. Lo, S. H. Ho, C. E. Chen, W. L. Chung, J. M. Shih *et al.*, *IEEE Electron Device Lett.* **32**(7), 847–849 (2011).

³W. H. Lo, T. C. Chang, C. H. Dai, W. L. Chung, C. E. Chen, S. H. Ho, O. Cheng, and C. T. Huang, *IEEE Electron Device Lett.* **33**(3), 303–305 (2012).

⁴Y. J. Kuo, T. C. Chang, P. H. Yeh, S. C. Chen, C. H. Dai, C. H. Chao, T. F. Young, O. Cheng, and C. T. Huang, *Thin Solid Films* **517**, 1715 (2009).

⁵Y. J. Kuo, T. C. Chang, C. H. Dai, S. C. Chen, J. Lu, S. H. Ho, C. H. Chao, T. F. Young, O. Cheng, and C. T. Huang, *Electrochem. Solid-State Lett.* **12**, H32 (2009).

⁶C. H. Dai, T. C. Chang, A. K. Chu, Y. J. Kuo, S. H. Ho, T. Y. Hsieh, W. H. Lo, C. E. Chen, J. M. Shih, W. L. Chung *et al.*, *Appl. Phys. Lett.* **99**, 012106 (2011).

⁷C. H. Dai, T. C. Chang, A. K. Chu, Y. J. Kuo, W. H. Lo, S. H. Ho, C. E. Chen, J. M. Shih, H. M. Chen, B. S. Dai *et al.*, *Appl. Phys. Lett.* **98**, 092112 (2011).

⁸C. H. Dai, T. C. Chang, A. K. Chu, Y. J. Kuo, Y. C. Hung, W. H. Lo, S. H. Ho, C. E. Chen, J. M. Shih, W. L. Chung *et al.*, *Thin Solid Films* **520**, 1511 (2011).

⁹W. H. Lo, T. C. Chang, J. Y. Tsai, C. H. Dai, C. E. Chen, S. H. Ho, H. M. Chen, O. Cheng, and C. T. Huang, *Appl. Phys. Lett.* **100**, 152102 (2012).

¹⁰M. B. Zahid, R. Degraeve, M. Cho, L. Pantisano, D. R. Aguado, J. Van Houdt, G. Groeseneken, and M. Jurczak, in *Reliability Physics Symposium* (2009), pp. 21–25.

¹¹W. J. Zhu and T. P. Ma, *IEEE Electron Device Lett.* **25**(2), 89–91 (2004).

¹²R. Chau, S. Datta, M. Doczy, B. Doyle, J. Kavalieros, and M. Metz, *IEEE Electron Devices Lett.* **25**(6), 408–410 (2004).

¹³H. Aozasa, I. Fujiwara, A. Nakamura, and Y. Komatsu, *Jpn. J. Appl. Phys., Part 1* **38**, 1441–1447 (1999).

¹⁴I. Lundström and C. Svensson, *J. Appl. Phys.* **43**, 5045 (1972).

¹⁵T. Wang, N. K. Zous, J. L. Lai, and C. Huang, *IEEE Electron Device Lett.* **19**(11), 411–413 (1998).

¹⁶W. C. Lee and C. Hu, *IEEE Trans. Electron Devices* **48**(7), 1366–1373 (2001).

¹⁷T. V. Perevalov, V. A. Gritsenko, S. B. Erenburg, A. M. Badalyan, H. Wong *et al.*, *J. Appl. Phys.* **101**, 053704 (2007).

¹⁸C. C. Yeh, T. P. Ma, N. Ramaswamy, N. Rocklein, D. Gealy, T. Graettinger, and K. Min, *Appl. Phys. Lett.* **91**, 113521 (2007).

¹⁹K. Xiong, J. Robertson, M. C. Gibson, and S. J. Clark, *Appl. Phys. Lett.* **87**, 183505 (2005).

²⁰S. H. Ho, T. C. Chang, C. W. Wu, W. H. Lo, C. E. Chen, J. Y. Tsai, H. P. Luo, T. Y. Tseng, O. Cheng, C. T. Huang *et al.*, *Appl. Phys. Lett.* **101**, 052105 (2012).